ELSEVIER

Physica A 284 (2000) 318–334

PHYSICA A

www.elsevier.com/locate/physa

A wire length minimization approach to ocular dominance patterns in mammalian visual cortex

Dmitri B. Chklovskii, Alexei A. Koulakov*

Sloan Center for Theoretical Neurobiology, The Salk Institute, La Jolla, CA 92037, USA

Received 8 February 2000

Abstract

The primary visual area (V1) of the mammalian brain is a thin sheet of neurons. Because each neuron is dominated by either right or left eye one can treat V1 as a binary mixture of neurons. The spatial arrangement of neurons dominated by different eyes is known as the ocular dominance (OD) pattern. We propose a theory for OD patterns based on the premise that they are evolutionary adaptations to minimize the length of intra-cortical connections. Thus, the existing OD patterns are obtained by solving a wire length minimization problem. We divide all the neurons into two classes: right- and left-eye dominated. We find that if the number of connections of each neuron with the neurons of the same class differs from that with the other class, the segregation of neurons into monocular regions indeed reduces the wire length. The shape of the regions depends on the relative number of neurons in the two classes. If both classes are equally represented we find that the optimal OD pattern consists of alternating stripes. If one class is less numerous than the other, the optimal OD pattern consists of patches of the underrepresented (ipsilateral) eye dominated neurons surrounded by the neurons of the other class. We predict the transition from stripes to patches when the fraction of neurons dominated by the ipsilateral eye is about 40%. This prediction agrees with the data in macaque and *Cebus* monkeys. Our theory can be applied to other binary cortical systems.

1. Introduction

In mammals inputs from the two eyes come together in the primary visual area (V1) which is a thin sheet of neurons. Neurons in V1 respond to the stimulation of the two eyes unevenly: they are either right or left-eye dominated. Accordingly, each neuron belongs to one of the two ocular dominance classes. The arrangement of neurons varies between different animals. In some species neurons belonging to different classes are

* Corresponding author.
E-mail address: akula@salk.edu (A.A. Koulakov).

0378-4371/00/$ - see front matter
PII: S0378-4371(00)00219-3

uniformly intermixed. In others the binary mixture of right- and left-eye-dominated neurons is segregated resulting in a system of alternating monocular regions. This system is known as the ocular dominance (OD) pattern [1].

Most theorists interested in the OD pattern [2,3] have been modeling its development. They succeeded in generating OD patterns of realistic appearance. However, several *why* rather than *how* questions remained unanswered. Why, from the functional point of view, do the OD patterns exist? Why do some mammalian species have OD patterns while others do not (like owl monkeys and adult marmosets [3])? Why do monocular regions have different appearances (stripes as opposed to patches) between different species and even between different parts of V1 within the same animal?

Mitchison [4] suggested an answer to the first question using the wiring economy principle [5–10]. The idea is that the evolutionary pressure to keep the brain volume to a minimum requires making the wiring (axons and dendrites) as short as possible, while maintaining function. In general, the function of a neuronal circuit specifies the connections between neurons (wiring rules). Therefore, the problem presented by the wiring economy principle is to find, for given wiring rules, the spatial layout of neurons that minimizes wire length. Then we can understand the existing layout of neurons as a solution to the wire length minimization problem.

We adopt the wiring economy principle and address the above questions by formulating and solving a wire length minimization problem. Neurons in V1 follow the principle of columnar organization which states that the properties of neurons remain the same perpendicular to the sheet [11]. Therefore, we consider a two-dimensional neuronal layer of uniform density. The number of the left-eye-dominated neurons is a fraction f_L of the total number, and f_R is a fraction of right-eye-dominated neurons ($f_L + f_R = 1$).

We consider only inter-neuronal connections which do not leave V1 because they constitute the majority of gray matter wiring [12–14]. We assume that each neuron receives synapses from N_s neurons dominated by the same eye and from N_o neurons dominated by the opposite eye. In other words, because synapses are unidirectional the resulting wiring rules require each neuron to get unidirectional connections from N_s neurons dominated by the same eye and from N_o neurons dominated by the opposite eye.

Given these wiring rules we look for an optimal layout of neurons which minimizes the total length of connections. Depending on the values of N_s, N_o, and f_L, optimal layout belongs to the one of the four phases shown in Fig. 1 where left-eye-dominated neurons are shown in black and right-eye-dominated neurons – in white. In the unsegregated *Salt and Pepper* phase right- and left-eye-dominated neurons are uniformly intermixed (Fig. 1a). The *Stripe* phase consists of alternating monocular stripes of neurons dominated by either eye (Fig. 1b). The *L-Patch* consists of the patches of the left-eye-dominated neurons surrounded by the right-eye-dominated neurons (Fig. 1c). The *R-Patch* consists of the patches of the right-eye-dominated neurons surrounded by the left-eye-dominated neurons (Fig. 1d). The segregated *Stripe, L-Patch*, and *R-Patch* phases dominate the phase diagram (see below).

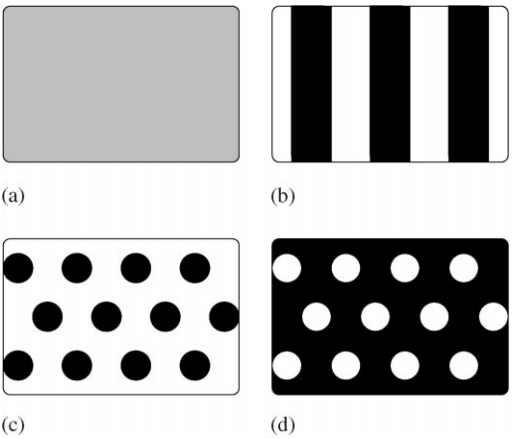

Fig. 1. Different appearances of the ocular dominance pattern. Left-eye-dominated neurons are black while right-eye-dominated neurons are white. (a) *Salt and Pepper* phase, uniformly intermixed left/right neurons. (b) *Stripe* phase, alternating monocular stripes. (c) *L-Patch* phase, circular left-eye islands in the right-eye sea. (d) *R-Patch* phase, circular right-eye islands in the left-eye sea.

Our approach differs from Mitchison's in that we drop the retinotopy requirement, i.e., the connection matrix in our approach (N_s and N_o) is independent on the position of the center of the visual field on retina. This implies that the mutual interaction between the ocular dominance pattern and the retinotopic map in weak. This simplification is supported by the existence of the receptive field scatter [15], random variation in the receptive field position between adjacent neurons. For example, in macaque retinotopy exists only on the scales greater than ≈ 1 mm [15], which exceeds the typical size of monocular regions. This implies that the position of the center of the receptive field of the neuron is not a well-defined quantity on the scales exceeding the characteristic dimension of the OD pattern. Hence, the selectivity of the local connections to retinotopy should be weak.

In the Discussion we compare our predictions with the data from macaque and Cebus monkeys and find good agreement. Also, we discuss simplifying assumptions made in the paper and possible ways to extend the theory.

2. Results

We present the central results of the paper on a phase diagram (Fig. 2) showing optimal phases for various ratios of same-eye to other-eye connections N_s/N_o and fractions of left-eye neurons f_L. If the numbers of same-eye and other-eye connections are equal, $N_s/N_o = 1$ then *Salt and pepper* phase is optimal. Otherwise, if $N_s/N_o \neq 1$ the wirelength is minimized by an OD pattern consisting of alternating monocular regions. The shape of these regions depends on the relative fraction of the left-eye-dominated neurons, f_L. When the numbers of neurons dominated by each eye are close, $f_L \approx f_R$,

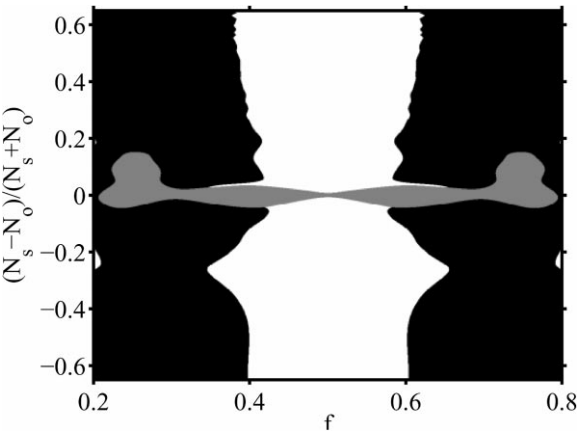

Fig. 2. Ocular dominance phase diagram calculated in the lattice model. Optimal phases are shown for various values of the relative difference between the same-eye and the other-eye connections $(N_s - N_o)/(N_s + N_o)$ and a fraction of left-eye neurons f. Range of the *Stripe* phase optimality is shown in white, *Patch* phase – in black, *Salt and Pepper* – in grey.

the *Stripe* phase is optimal. When the fraction of left-eye (right-eye)-dominated neurons drops below a critical value $f_c \approx 0.4$ the *L-Patch* (*R-Patch*) phase becomes optimal. Our predictions of the critical value agree with the data from macaque and Cebus monkeys.

In the following section we formulate a wiring problem on a lattice. For small N_s and N_o we solve it analytically while for large N_s and N_o we solve it numerically. Results are shown in Fig. 2. Next, we introduce a continuous formulation of the problem. We prove that *Salt and Pepper* is an optimal layout when $N_s = N_o$. Then we show that for $N_s \neq N_o$ segregation of neurons according to their OD reduces wire length. We calculate in perturbation theory the wire length for *Stripe* and *Patch* phases and find the range of parameters for the optimality of each phase. Perturbation theory provides an analytical treatment of neuronal clustering so common throughout the nervous system. The calculated phase diagram is similar to that obtained in the lattice model.

3. Lattice model

Although the arrangement of neurons in cerebral cortex is anything but grid-like we can understand many features of the neuronal layout by studying lattice models. These models compensate in clarity and computability what they lack in realism. Of course, we need to make sure that the results are independent of the particular choices of lattice parameters (for example the number of nearest neighbors).

We consider arranging a large number of neurons on a two-dimensional square lattice. Each site must be occupied by either left- or right-eye-dominated neuron. The number of the left-eye-dominated neurons is a fraction f_L of the total number of

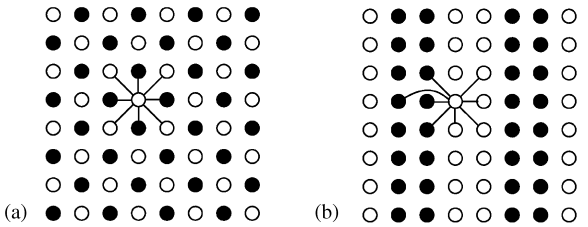

Fig. 3. Ocular dominance patterns for $f_L = \frac{1}{2}$ and $N_s = N_o = 4$. (a) A realization of the *Salt and Pepper* phase gives minimal wire length ($l \approx 9.67$ lattice constants per neuron). (b) A realization of the *Stripe* phase is suboptimal ($l \approx 10.24$).

neurons and f_R is a fraction of right-eye-dominated neurons. The problem is to find a layout which minimizes the total length of wiring specified by the following rule. Each left-eye neuron has unidirectional connections with N_s left-eye neurons and with N_o right-eye neurons. Each right-eye neuron has unidirectional connections with N_s right-eye neurons and with N_o left-eye neurons. Unidirectionality of connections means that connecting neuron A to neuron B, does not necessarily imply that neuron B connects to neuron A. The motivation for this rule comes from the unidirectional properties of synapses in the brain.

Because we attempt to minimize wire length we assume that for a given layout the connections are established optimally. Thus, the problem is reduced to comparing optimal wiring for various layouts. Therefore, we will assume that each neuron makes the shortest possible connections satisfying wiring rules.

3.1. Small numbers of connections per neuron

We start by finding optimal layouts for three illustrative examples of wiring rules with small numbers of connections, N_s and N_o. We caution the reader that because of the small numbers of connections phase assignments may seem arbitrary. These examples are chosen to illustrate our main results which will be confirmed both in the lattice model with large N_s and N_o later in this section and in the continuous model (Section 4).

For the first two examples we set equal numbers of left- and right-dominated neurons, $f_L = f_R = \frac{1}{2}$. In the first example, each neuron connects with equal numbers of the same-eye and other-eye neurons, $N_s = N_o = 4$. Then the optimal layout is the "chess board" of left/right neurons, Fig. 3a. This layout is a realization of the *Salt and Pepper* phase (Fig. 1a) because each neuron has an equal number of left and right neurons among its immediate neighbors. To calculate the length of connections per neuron, l, we notice that in this layout all neurons have the same pattern of connections. By considering one of them (Fig. 3a) we find that $l = 4 + 4\sqrt{2} \approx 9.67$. This layout is optimal because each neuron makes all of its connections with immediate neighbors.

A suboptimal layout for the same wiring rules is illustrated by a realization of the *Stripe* phase (Fig. 3b). In this layout each neuron has the same pattern of connections

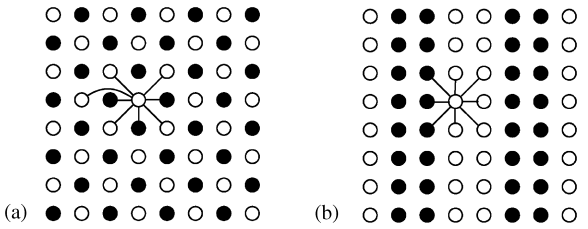

Fig. 4. Ocular dominance patterns for $f_L = \frac{1}{2}$ and $N_s = 5$, $N_o = 3$. (a) A realization of the *Salt and Pepper* is suboptimal ($l \approx 10.24$). (b) A realization of the *Stripe* phase gives minimal wire length ($l \approx 9.67$).

up to a mirror reflection. By considering one of them (Fig. 3b) we find $l = 6 + 3\sqrt{2} \approx 10.24$, greater than $l \approx 9.67$ for the *Salt and Pepper* phase. Here each neuron has among its immediate neighbors only three other-eye neurons, while the wiring rules require connecting with four other-eye neurons. A connection to a more distant neighbor is longer making the layout suboptimal. We confirm the optimality of the *Salt and Pepper* phase for $N_s = N_o$ for large N_s, N_o both numerically and analytically.

In the second example, each neuron connects with more same-eye than other-eye neurons: $N_s = 5$, $N_o = 3$. Then a realization of the *Salt and Pepper* phase, Fig. 4a is not optimal anymore. The length of connections per neuron is $l \approx 10.24$, while the *Stripe* phase, Fig. 4b gives $l \approx 9.67$. The *Salt and Pepper* phase loses in wiring efficiency because there are not enough same-eye neurons among immediate neighbors and connections with more distant neighbors are needed. The *Stripe* phase, Fig. 4b rectifies this inefficiency by having each neuron make connections only with immediate neighbors. Thus, clustering of same-eye neurons is advantageous if each neuron connects more with the same-eye than with the other-eye neurons.

In the third example, we use the same wiring rules ($N_s = 5$, $N_o = 3$) but take different numbers of left/right neurons, $f_L = 1/4$, $f_R = 3/4$. The realizations of the *Salt and Pepper* phase is shown in Fig. 5a and of the *Stripe* phase in Fig. 5b. In these layouts, different neurons have different patterns of connections. To find the wiring length per neuron we average over different patterns and find for the *Salt and Pepper* phase $l \approx 11.26$ and for the *Stripe* phase $l \approx 11.49$. A more efficient layout is the *L-Patch* phase (Fig. 5c) where $l \approx 10.67$. Although we cannot prove that the *L-Patch* phase is optimal, this seems likely. Thus, the optimal shape of monocular regions depends on the relative numbers of left/right neurons.

3.2. Large numbers of connections per neuron

Lattice models with small numbers of connections per neuron yield quick results good for illustration purposes. However, they are difficult to generalize to the wiring rules with large numbers of connections more appropriate for cortical circuits where each neuron connects with $\approx 10^4$ neurons. Therefore, we study lattice problems with large numbers of connections per neuron.

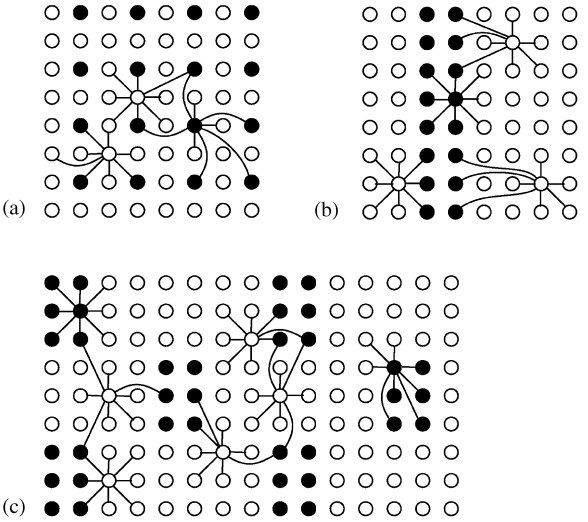

Fig. 5. Ocular dominance patterns for $f_L = \frac{1}{4}$ and $N_s = 5$, $N_o = 3$. Realizations of the (a) *Salt and Pepper* ($l \approx 11.26$) and (b) *Stripes* ($l \approx 11.49$) are suboptimal. (c) A realization of the *L-Patch* phase gives minimal wire length ($l \approx 10.67$).

When the number of connections per neuron is much greater than the number of nearest neighbors, the effect of the discreteness of the lattice on the results is negligible. In particular, for a given fraction f_L and ratio N_s/N_o only the periodicity of the optimal layout depends on the N_o. Thus, the solution of the wire length minimization problem for one value of N_o can be generalized to other problems with the same f_L and N_s/N_o.

We solve the wire length minimization problem using the following numerical algorithm. We fix the values of f_L and N_s/N_o. We use lattice sizes up to 300×300 sites and $N_o = 240$. We consider neuronal layouts belonging to several phases: *Salt and Pepper*, *Stripe*, *L-(R) Patch* (both triangular and square lattice), *Checkerboard* (only for $f_L = \frac{1}{2}$). For each phase we find the optimal period which minimizes wire length. Then we compare wire length in the optimal layouts of different phases. We plot the optimal phases for various values of f_L and N_s/N_o on the phase diagram (Fig. 2). These results were discussed above.

4. Continuous model

In this section we study the limit when N_s and N_o are very large. Instead of considering each receiving connections neuron separately it makes sense to treat them as a mixture of two "liquids", the left- and right-eye ones, having continuous in space densities. Segregation of such a mixture implies that the OD structure is formed.

4.1. The model

In this subsection, we will assume that the neuron configuration represented by the neuron densities is given. It can be any arbitrary configuration, including *Salt and Pepper*, *Stripes*, or *Patches*. For the given neuron densities we draw the connections between the cells which

- satisfy the wiring rules (N_s same and N_o other neuron connection have to be established); and
- minimize the total wire length.

In the end of the subsection, we calculate the wire length for the *Salt and Pepper* configuration.

We consider the mixture of neurons of two types: dominated by the left and right eyes. We assume that the neurons are located in the plane. This assumption is based on the fact that the OD remains constant in the direction perpendicular to the cortex surface. The variables of the problem can therefore be considered functions of the remaining two coordinates, $\mathbf{r}$.

Instead of considering each individual cell we characterize the neuron configuration by continuous local variables. We define the local density of neurons dominated by the right eye $n_R(\mathbf{r})$ as the average density in a square containing sufficiently large number of cells (> 10), yet small compared to the typical spatial scales of the configuration ($\sim$ 1 mm). Similarly $n_L(\mathbf{r})$ is the local density of cells dominant by the left eye. Although both $n_R(\mathbf{r})$ and $n_L(\mathbf{r})$ can vary in space, the total density of neurons $n_0 \equiv n_R(\mathbf{r}) + n_L(\mathbf{r})$ is a constant, independent of the position in the cortex.

In our model $n_R(\mathbf{r})$ and $n_L(\mathbf{r})$ completely define the neuron configuration. For example the *Salt and Pepper* configuration, in which the densities of right- and left-eye neurons are uniform, can be defined as follows:

$$n_R(\mathbf{r}) \equiv \bar{n}_R = f_R n_0 \,,$$

$$n_L(\mathbf{r}) \equiv \bar{n}_L = f_L n_0 \,,$$

$$\bar{n}_R + \bar{n}_L = n_0 \,. \tag{1}$$

Here f_R is defined as the fraction of the right-eye neurons with respect to the total number of cells (in general not $\frac{1}{2}$).

Having defined the neuron configuration by fixing the densities $n_R(\mathbf{r})$ and $n_L(\mathbf{r})$ we proceed to establishing the connections between cells. Two requirements have to be taken into account. First, we have to satisfy the wiring rules. Second, for given densities $n_R(\mathbf{r})$ and $n_L(\mathbf{r})$ the total length of connections has to be minimum. Consider a pattern of connections from a neuron dominated, for example, by the right eye. Consider also the region in the cortex it is connected to. There are in fact two such regions, for the right- and left-eye connections. We claim that each of these regions is a disc. To prove this, notice that if the connections are produced with neurons outside of this disk rather than inside the wire length is increased. This is inconsistent with the requirement of

the optimum wiring for a given configuration. We denote the radii of these two disks $R_{RR}(\mathbf{r})$ and $R_{RL}(\mathbf{r})$, implying the radii of right-eye neuron at point $\mathbf{r}$ connection regions to the right-eye and left-eye cells correspondingly. Similar quantities can be introduced for the left-eye neurons at point $\mathbf{r}$, i.e., $R_{LR}(\mathbf{r})$ and $R_{LL}(\mathbf{r})$. We introduce the index notation $i=\{R,L\}$. Then the four radii discussed can be collapsed into one notation $R_{ik}(\mathbf{r})$, standing for the radius of the connection region for the neuron of OD i at point $\mathbf{r}$ to the cells of OD k. The radius can be determined from the wiring rules (N_s and N_o connections to the cells of the same and other OD, respectively, have to be established):

$$N_{ik}=\int_{|\mathbf{r}-\mathbf{r}'|\leqslant R_{ik}(\mathbf{r})} \mathrm{d}\mathbf{r}' n_k(\mathbf{r}')\,. \tag{2}$$

Here the elements of matrix N_{ik}, $i=\{R,L\}$ are equal to N_s if $i=k$ and N_o otherwise.

It is now possible to determine the total connection length in the cortex $\mathscr{L}$. To this end we add up the lengths of the connections of individual neurons $L_{ik}(\mathbf{r})$ over the whole area:

$$\mathscr{L}=\int \mathrm{d}\mathbf{r} \sum_{i,\,k=R,\,L} n_i(\mathbf{r})L_{ik}(\mathbf{r})\,, \tag{3}$$

where

$$L_{ik}(\mathbf{r})=\int_{|\mathbf{r}-\mathbf{r}'|\leqslant R_{ik}(\mathbf{r})} \mathrm{d}\mathbf{r}' n_k(\mathbf{r}')|\mathbf{r}-\mathbf{r}'|\,. \tag{4}$$

The last factor in this expression is the connection length as a function of separation $|\mathbf{r}-\mathbf{r}'|$ between neurons. In principle, cost function may not be a linear function of separation. This would be the case if the axon diameter changed with distance. However, we take it to be linear assuming no substantial change of the average axonal diameter as a function of length. Eqs. (2)–(4) define our model completely.

Using Eq. (3) we calculate the wire length for the homogeneous *Salt and Pepper* configuration. To this end we substitute the densities given by Eq. (1) into (2) to find

$$R_{ik}^{SP}=\sqrt{\frac{N_{ik}}{\pi n_k}}\,. \tag{5}$$

Then using Eqs. (3) and (4) we obtain

$$L_{ik}=\frac{2}{3}R_{ik}^{SP}N_{ik} \tag{6}$$

and finally

$$\mathscr{L}^{SP}=\frac{2A}{3}\left[\sqrt{\frac{N_s^3}{\pi}}(\sqrt{n_R}+\sqrt{n_L})+\sqrt{\frac{N_o^3}{\pi}}\left(\frac{n_R}{\sqrt{n_L}}+\frac{n_L}{\sqrt{n_R}}\right)\right]\,, \tag{7}$$

where A is the total area of the cortex.

In the next subsection, we show that wire length can be reduced with respect to (7) by introducing a small inhomogeneity into the neuron densities n_R and n_L. To this end we treat our model (2)–(4) in the framework of the perturbation theory.

4.2. Instability of the uniform state leads to the formation of patterns

The purpose of this subsection is to study structures that do not deviate far from the uniform *Salt and Pepper* configuration discussed in the previous subsection. Because we have solved the uniform configuration exactly, the configurations which are not far from it are also treatable by the perturbation theory analysis, i.e., expansion of the wire length (3) in terms of the deviation of densities of right- and left-eye neurons from the constant. This treatment determines which of the inhomogeneous phases (*Stripe* or *Patch*) is optimum. Also, comparison with the numerical results shows that the perturbation theory results hold even for big differences in density.

We therefore consider a small repositioning of neurons, leading to the deviation of densities from constant $\delta n(\mathbf{r})$. Because $n_R + n_L = n_0$

$$n_R(\mathbf{r}) = \bar{n}_R + \delta n(\mathbf{r}) ,$$

$$n_L(\mathbf{r}) = \bar{n}_L - \delta n(\mathbf{r}) . \tag{8}$$

As this is only rearrangement the average of $\delta n(\mathbf{r})$ over the entire volume $\overline{\delta n(\mathbf{r})}$ is zero, i.e., the total number of left- and right-eye neurons is not changed by the perturbation. We then substitute these functions into our model (2)–(4) and calculate expansion of the wire length in the Taylor series in $\delta n(\mathbf{r})$. It has the form

$$\mathscr{L} = \mathscr{L}^{SP} + \mathscr{L}^{(1)} + \mathscr{L}^{(2)} + \cdots , \tag{9}$$

where $\mathscr{L}^{SP}$ is given by Eq. (7), $\mathscr{L}^{(1)} \propto \delta n$, $\mathscr{L}^{(2)} \propto \delta n^2$ are the first- and the second-order corrections to the wire length. From the condition $\overline{\delta n(\mathbf{r})} = 0$ it follows that $\mathscr{L}^{(1)} = 0$. The second-order correction to the wire length is

$$\mathscr{L}^{(2)} = \int \mathrm{d}\mathbf{r}\,\mathrm{d}\mathbf{r}' \sum_{i,k=R,L} R_{ik}^{SP} \times \{U_{1ik}(\mathbf{r}-\mathbf{r}')\delta n_i(\mathbf{r})\delta n_k(\mathbf{r}') + U_{2ik}(\mathbf{r}-\mathbf{r}')\delta n_k(\mathbf{r})\delta n_k(\mathbf{r}')\} . \tag{10}$$

Here $\delta n_i(\mathbf{r})$ is the perturbation of density of neurons of ith dominance ($\delta n_R = \delta n$, $\delta n_L = -\delta n$,) and

$$U_{1ik}(\mathbf{r}) = \theta(R_{ik}^{SP} - |\mathbf{r}|)\left(\frac{|\mathbf{r}|}{R_{ik}^{SP}} - 1\right) , \tag{11}$$

$$U_{2ik}(\mathbf{r}) = \frac{1}{4\pi(R_{ik}^{SP})^2}\int \mathrm{d}\mathbf{r}''\theta(R_{ik}^{SP} - |\mathbf{r}-\mathbf{r}''|)\theta(R_{ik}^{SP} - |\mathbf{r}''|) , \tag{12}$$

where $\theta(x) = 1$, if $x \geqslant 0$, and $\theta(x) = 0$, if $x < 0$. Because U_{2ik} has the geometrical interpretation of the overlap between two disks

$$U_{2ik}(\mathbf{r}) = \left[\frac{1}{2\pi}\arccos\left(\frac{|\mathbf{r}|}{2R_{ik}^{SP}}\right) - \frac{|\mathbf{r}|}{4\pi R_{ik}^{SP}}\sqrt{1-\left(\frac{|\mathbf{r}|}{2R_{ik}^{SP}}\right)^2}\right]\theta(2R_{ik}^{SP} - |\mathbf{r}|) . \tag{13}$$

Using Eq. (8) we express the second-order correction to the wire length (10) as a pairwise density–density interaction

$$\mathscr{L}^{(2)} = \int \mathrm{d}\mathbf{r}\,\mathrm{d}\mathbf{r}'\,\delta n(\mathbf{r})\mathscr{U}(\mathbf{r}-\mathbf{r}')\delta n(\mathbf{r}')\,, \tag{14}$$

where the "interaction potential" $\mathscr{U}(\mathbf{r})$ is given by

$$\mathscr{U}(\mathbf{r}) = \mathscr{U}_1(\mathbf{r}) + \mathscr{U}_2(\mathbf{r})\,, \tag{15}$$

$$\mathscr{U}_1 = U_{1RR} + U_{1LL} - U_{1RL} - U_{1LR}\,, \tag{16}$$

$$\mathscr{U}_2 = U_{2RR} + U_{2LL} + U_{2RL} + U_{2LR}\,. \tag{17}$$

We notice that expression (14) is similar to the Hamiltonian used by Cowan and Friedman [16], which corresponds to Swindale [17] learning rules. The advantage of our approach is that we derive this expression from a single principle without assuming a particular form of "interaction potential". In addition, we go on to solve this expression analytically. This allows us to map out a phase diagram which relates the ocular dominance pattern to biologically measurable connection rules without appealing to "Mexican hat" connection weights.

We convert Eq. (14) into Fourier space using the property of a convolution

$$\mathscr{L}^{(2)} = \int \frac{\mathrm{d}\mathbf{q}}{(2\pi)^2}\tilde{\mathscr{U}}(\mathbf{q})|\delta\tilde{n}(\mathbf{q})|^2\,, \tag{18}$$

where $\tilde{\mathscr{U}}(\mathbf{q})$ and $\delta\tilde{n}(\mathbf{q})$ are Fourier transforms of the "interaction potential" and the perturbation of density, respectively. The Fourier transform of a function $f(\mathbf{r})$ is defined as $\tilde{f}(\mathbf{q}) = \int \mathrm{d}\mathbf{r}\,f(\mathbf{r})\exp(-\mathrm{i}\mathbf{q}\mathbf{r})$, where $\mathrm{i} = \sqrt{-1}$ is the imaginary unity. Eq. (18) is the central result of this subsection.

Function $\tilde{\mathscr{U}}(\mathbf{q})$ determines the changes in the total wire length due to the deviation of the neuron density from constant. For example, if the perturbation of density has the form of plane wave ($\delta n = a\cos(\mathbf{q}_0\mathbf{r})$), the change in the total wire length is proportional to $\tilde{\mathscr{U}}(\mathbf{q}_0)a^2$. Thus if $\tilde{\mathscr{U}}(\mathbf{q})$ is negative at certain q_0, such a perturbation *decreases* the total wire length. It is therefore advantageous from the point of view of wire length economy to create a perturbation of density at this wave vector. In this case the uniform *Salt and Pepper* configuration ($\delta n = 0$) is unstable with respect to the formation of the OD patterns. Hence, negative function $\tilde{\mathscr{U}}(\mathbf{q})$ indicates the formation of an OD pattern.

We therefore analyze the conditions at which the function has negative values. Two statements can be made in this respect. First, assume that $N_s = N_o$. Then $\tilde{\mathscr{U}}(\mathbf{q})$ is never negative. Indeed in this case $U_{1RR} \equiv U_{1LR}$ and $U_{1RL} \equiv U_{1LL}$ (see Definition (11) and Eq. (5)). Therefore, according to (16), $\mathscr{U}_1 \equiv 0$. At the same time $U_{2ik}(\mathbf{q}) \geqslant 0$ as a Fourier transform of the convolution of two disks. Hence if $N_s = N_o$, $\mathscr{U}(\mathbf{q}) \equiv \mathscr{U}_2(\mathbf{q}) \geqslant 0$. This implies that *Salt and Pepper* is optimum if $N_s = N_o$. Second, consider $\tilde{\mathscr{U}}(\mathbf{q})$ at $f_R = f_L = \frac{1}{2}$ and arbitrary $N_s \neq N_o$. In this case $\tilde{\mathscr{U}}(\mathbf{q})$ always has negative values. This means that on the line of equal right-left eye occupancy $f_R = f_L = \frac{1}{2}$ the OD patterns are *always* optimum, except for the point $N_s = N_o$. We do not give the proof of this property due to the space limitations.

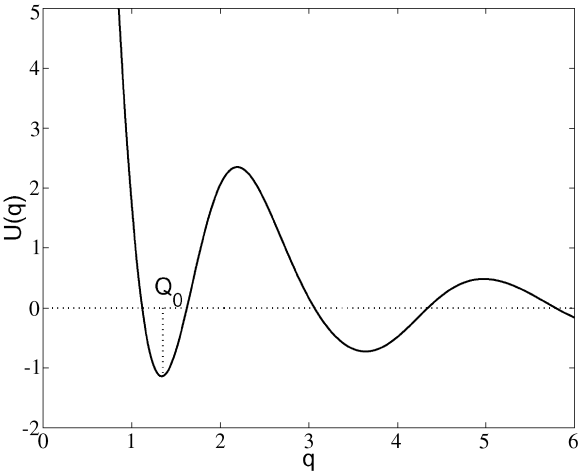

Fig. 6. Function $\tilde{\mathscr{U}}(\mathbf{q})$ calculated numerically for $N_s = 10$, $N_o = 7$, $f_R = \frac{1}{2}$, and $n_0 = 1$. The value of wave vector corresponding to the most negative value of the function is denoted Q_0.

To illustrate these properties we show an example of $\tilde{\mathscr{U}}(\mathbf{q})$ in Fig. 6. The function obviously has negative values, signifying instability and an OD pattern formation. The instability is strongest at the wave vector corresponding to the most negative value of $\tilde{\mathscr{U}}(\mathbf{q})$. Indeed, creating the structure at this wave vector reduces the total wire length most effectively. We predict therefore the spatial period of the OD pattern. For the case $N_s \approx N_o$ shown in Fig. 6 ($N_s = 10$ and $N_o = 9$) function $\tilde{\mathscr{U}}(\mathbf{q})$ reaches the most negative value at

$$Q_0 \approx \frac{3}{R_{RR}^{SP}} \approx \frac{3}{R_{RL}^{SP}} \,. \tag{19}$$

The spatial period of the OD pattern is therefore

$$\Lambda = \frac{2\pi}{Q_0} \approx 2R_{RR}^{SP} \approx 2R_{RL}^{SP} \,. \tag{20}$$

In other words, it is approximately equal to the diameter of the disc of connections.

4.3. Competition between the Stripe and Patch phases

Next, we use the perturbation theory to calculate approximately the wire lengths of different OD structures. Because the structures are periodic the integral in Eq. (18) can be reduced to the sum over the reciprocal lattice vectors $\mathbf{Q}$:

$$\mathscr{L}^{(2)} = \frac{1}{A} \sum_{\mathbf{Q} \neq 0} \tilde{\mathscr{U}}(\mathbf{Q}) |\delta\tilde{n}(\mathbf{Q})|^2 \,, \tag{21}$$

where A is the total area of the system. Different OD structures have different sets of $\mathbf{Q}$ and $\delta\tilde{n}(\mathbf{Q})$. For example, for *Stripes* $Q_x = 2\pi n/\Lambda$, $Q_y = 0$, where $n = \pm 1, \pm 2, \ldots$ and

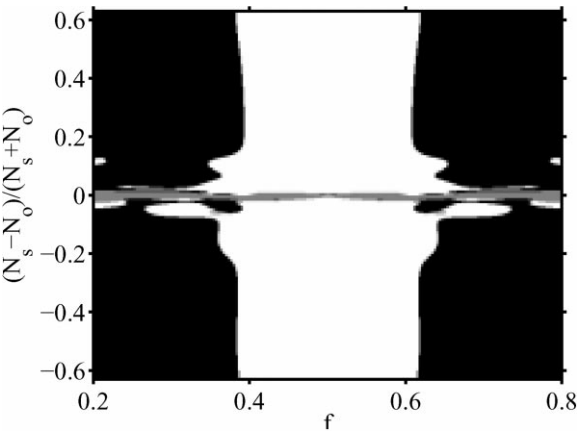

Fig. 7. Ocular dominance phase diagram calculated in perturbation theory. Range of the *Stripe* phase optimality is shown in white, *Patch* phase – in black, *Salt and Pepper* – in grey. The axes are labeled similar to Fig. 2.

Λ is the spatial period of the structure. The Fourier transform of density

$$\delta\tilde{n}_{\text{Stripes}}(\mathbf{Q}) = \frac{2A}{\Lambda|\mathbf{Q}|}\sin\left(\frac{f_R|\mathbf{Q}|\Lambda}{2}\right) . \tag{22}$$

For the triangular lattice of *Patches* $Q_x = Q_0(l\sqrt{3}/2)$, $Q_y = Q_0(k + l/2)$, with $l,k = \pm1, \pm2, \ldots$ and $Q_0 = 4\pi/\Lambda\sqrt{3}$, where Λ is the lattice spacing. The Fourier transform of density

$$\delta\tilde{n}_{\text{Patches}}(\mathbf{Q}) = \frac{2A}{\Lambda|\mathbf{Q}|}\sqrt{\frac{2\pi f_R}{\sqrt{3}}}\sin\left(|\mathbf{Q}|\Lambda\sqrt{\frac{f_R\sqrt{3}}{2\pi}}\right) . \tag{23}$$

Based on Eqs. (21)–(23) we compare different OD structures and generate the phase diagram similar to one given in the introduction (see Fig. 7).

Figs. 2 and 7 have many similar features. First, the diagram is symmetric with respect to the line $f_R = \frac{1}{2}$. This is a consequence of the left-right eye symmetry of the general wire length functional (3) inherited by the second-order functional (18). The reason for the existence of such a symmetry is interchangeability of left and right eyes inherent to this model. If, for instance, in a given configuration one relabels left-eye neurons into the right-eye ones and vice versa, the wire length does not change.

Second, the *Salt and Pepper* phase occupies a stripe around the line $N_s = N_o$. The width of this line is given by $|N_s - N_o| < 0.01N_s$. This is the result of the above-mentioned stability of *Salt and Pepper* on the line $N_s = N_o$. As it is shown by the diagram, the stability extends into some region around this line.

Third, there is a transition between *Stripes* and *Patches* at $f_R \approx 0.4$ and 0.6. The region on the diagram corresponding to $0.4 < f_R < 0.6$ is almost completely occupied by the *Stripes* while the rest of the diagram ($f_R < 0.4$ and $f_R > 0.6$) by the *Patches*.

We explain this in the framework of the perturbation theory. The main contribution to Eq. (21) comes from the terms with the smallest $|\mathbf{Q}|$. This happens because both $\tilde{\mathscr{U}}(\mathbf{Q})$ and $\tilde{n}(\mathbf{Q})$ decay very fast with the increase of $|\mathbf{Q}|$. *Stripes* and *Patches* can approximately be compared using only the terms with the smallest $|\mathbf{Q}| \equiv Q_0$. The two solutions have equal wire length if

$$2\tilde{\mathscr{U}}(Q_0)|\delta\tilde{n}_{\text{Stripes}}(Q_0)|^2 = 6\tilde{\mathscr{U}}(Q_0)|\delta\tilde{n}_{\text{Patches}}(Q_0)|^2 , \tag{24}$$

where factors 2 and 6 are the numbers of the smallest wave length harmonics in the *Stripe* and *Patch* phases, respectively. Using Eqs. (22) and (23) to solve the latter equation for f_R we obtain numerically for the filling factor of the transition $f_R \approx 0.4$. Due to the mentioned left–right eye symmetry of the model similar transition occurs at $f_R = 1 - 0.4 = 0.6$.

We would like to notice finally that comparison of the perturbation theory to exact calculations shows that the former works well even if the deviation of the density from constant is not small ($\sim 0.5n_0$). Such a comparison shows that $([\mathscr{L} - \mathscr{L}^{SP}] - \mathscr{L}^{(2)})/\mathscr{L}^{(2)} < 5\%$. In addition, the perturbation theory provides a framework to understand numerous qualitative features of the phase diagram discussed above.

Von der Malsburg [18], has surmised that there is a phase transition between *Patches* and *Stripes* driven by the cost of the left/right eye boundary. However, he did not address different numbers of connections with same vs. other-eye neurons and made several different assumptions (e.g. fixing the periodicity of the pattern). Thus, our results offer a more complete description of the OD patterns while relying only on one principle – wire length minimization.

5. Discussion

5.1. Comparison with experiment

Our theory relates the properties of the neural circuit to the neuronal layout. In particular, the phase diagram relates the relative fractions of neurons, f_R, and of connections, N_s/N_o, to the appearance of the OD pattern. Ideally, this theory could be tested by measuring these numbers experimentally and comparing the observed OD pattern to the one predicted by the phase diagram. However, a direct measurement of N_s/N_o is not available yet and one can only surmise that it is greater than one.

In the mean time we can test some predictions of our model which are independent of the ratio N_s/N_o. Fig. 1 shows that the transition from the *Stripe* and the *L-Patch* (*R-Patch*) phase takes place when $f_R \approx 0.4$ (or $f_L \approx 0.4$) for a wide range of N_s/N_o. This number can be compared with the experimentally observed value of f_R at which the transition occurs. The statement that the *Patch* phase becomes optimal when one eye prevails is, indeed, non-trivial since there may be a system of alternating wide and narrow monocular stripes instead.

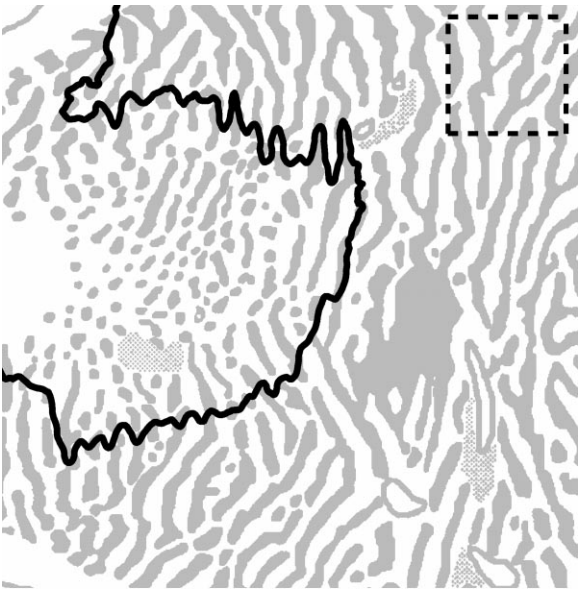

Fig. 8. Transition between the *Stripe* and *Patch* phases occurs at theoretically predicted value of f_R. Shown is a fragment of the macaque ocular dominance pattern from Horton and Hocking, 1996 [22]. Neurons dominated by the right eye are grey and neurons dominated by the left eye are white. Black contours correspond to the value $f_R = 0.4$ averaged over a window equal to the one shown by the dashed square. The side of the square is equal to 5.8 mm and is chosen to be much larger than the OD period (≈ 1 mm) and much smaller than the characteristic size of OD variation. Transition from *Stripe* to *Patch* phase visually coincides with the black contour.

We test our result on the data from macaque and *Cebus* monkey. The relative area occupied by the right/left eye depends on the location in V1. In the part of V1 corresponding to the center of the visual field both eyes are represented equally, i.e., $f_R \approx 0.5$. In agreement with the phase diagram, the OD pattern consists of stripes. In contrast, in the area corresponding to the periphery of the visual field one of the eyes (ipsilateral) becomes underrepresented. This occurs because some part of the image is occluded for the ipsilateral eye by the nose of the animal. Therefore $f_R < \frac{1}{2}$ there (if the right eye is ipsilateral). In such areas the OD pattern becomes patchy (see Fig. 8), just as expected from the phase diagram. We verify the location of the transition by using the following algorithm. We find f_R for each point of the pattern by calculating the relative area occupied by the left/right regions in a window centered on that point and a few OD periods wide (dashed lines in Fig. 8). Then we draw a contour corresponding to $f_L = 0.4$ (Fig. 8). Next, we check visually whether the location of this contour is close to the transition from *Stripes* to *Patches*. Indeed, the large black contour in Fig. 8 coincides with the transition indicating good agreement.

In *Cebus* monkey the OD pattern has a similar transition [19]. For monkey CO6L from Rosa et al. [19] we determine visually that along the horizontal meridian the

transition occurs at the eccentricity of 20–40°. According to the plot of the relative representations given in Rosa et al. [19], f_R changes in the range 0.32–0.42 at these eccentricities. Our prediction of $f_R = 0.4$ falls into this interval. For the upper 45° meridian of the same monkey the transition occurs at the eccentricity of 30–40° or at filling fractions 0.33–0.43. Again, the predicted value belongs to this interval. We conclude that this data agrees with our predictions although a more precise measurement would be helpful.

In cats the OD patterns resemble *Patches*. In this case our theory implies that one eye should be underrepresented. In fact, Shatz and Stryker [20] reported that the filling fraction of the ipsilateral eye in the entire cat V1 is smaller than 0.5. This may explain the existence of *Patches* in cat V1. However, other authors Anderson et al. [21] claimed that both eyes are represented almost equally. More precise measurements of the ocular dominance are needed to make a conclusive judgement.

5.2. Further development of the theory

Next, we elaborate on several simplifying assumptions made in the paper. Although these assumptions should not affect our conclusions significantly, they are worth further exploration.

First, the transition between *Stripes* and *Patches* may be more complex than discussed. We considered only two candidate phases: *Stripes* and a triangular lattice of circular *Patches*. It is possible that some intermediate phases become optimal near the transition. For example, Fig. 8 hints that parallel chains of elongated *Patches* may give more efficient wiring. This would slightly modify our phase diagram.

Second, we based our theory on looking for an optimal layout of neurons which minimizes total wire length. The considered structures are, therefore, regular and periodic. However, developmental noise may lead to fluctuations in the OD pattern which reduce slightly its wiring efficiency. Although actual OD patterns contain such fluctuations we do not know whether these are due to suboptimal wiring or variations in the wiring rules from point to point.

Different phases may have different stability in respect to noise. Judging from the data, the *Stripe* phase holds up well on the scale of a few periods. The *Patch* phase, however, does not show a regular triangular lattice. We think that this is because of a relatively small difference in wire length between the triangular and the square lattice of *Patches*. (It is about 0.5% of the total wire length, compared to 2% difference between *Stripes* and *Patches* for the upper left part of the phase diagram.)

Third, our theory can be expanded to address the interaction between different maps. Variables of other maps can enter the expression for the total wire length (Eq. (3)) through additional values of indices i and k, which so far reflect ocular dominance. Moreover, these indices can become continuous variables if the sums in (3) are replaced by integrals. This would be appropriate for including interactions with retinotopic and orientational selectivity maps.

Fourth, we applied our theory to the OD patterns as the best-studied structure. Since our model is based on minimal assumptions, it can be applied to other binary structures such as cytochrome oxidase blobs.

In conclusion, we explained the OD patterns in mammalian V1 by minimizing wire length given general functional considerations. Good agreement with experiment lends strong support to the notion that OD structures are adaptations to reduce intra-cortical wiring.

References

[1] T.N. Wiesel, D.H. Hubel, D.M. Lam, Autoradiographic demonstration of ocular-dominance columns in the monkey striate cortex by means of transneuronal transport, Brain Res. 79 (1974) 273–279.
[2] E. Erwin, K. Obermayer, K. Schulten, Models of orientation and ocular dominance columns in the visual cortex: a critical comparison, Neural Comput. 7 (1995) 425–468.
[3] N.V. Swindale, The development of topography in the visual cortex: a review of models, Network: Comput. Neural Systems 7 (1996) 161–247.
[4] G. Mitchison, Neuronal branching patterns and the economy of cortical wiring, Proc. Roy. Soc. London B Biol. Sci. 245 (1991) 151–158.
[5] S.Ry. Cajal, Histology of the Nervous System, Oxford University Press, New York, 1995, pp. 1–805.
[6] J.M. Allman, J.H. Kaas, The organization of the second visual area (V II) in the owl monkey: a second order transformation of the visual hemifield, Brain Res. 76 (1974) 247–265.
[7] A. Cowey, Cortical maps and visual perception: the Grindley Memorial Lecture, Quart. J. Exp. Psychol. 31 (1979) 1–17.
[8] C. Cherniak, Local optimization of neuron arbors, Biol. Cybern. 66 (1992) 503–510.
[9] M.P. Young, Objective analysis of the topological organization of the primate cortical visual system, Nature 358 (1992) 152–155.
[10] D.B. Chklovskii, C.F. Stevens, Wiring optimization in the brain, Neural Information Processing Systems (1999).
[11] V.B. Mountcastle, J. Neurophysiol. 20 (1957) 408–434.
[12] S. LeVay, C.D. Gilbert, Laminar patterns of geniculocortical projection in the cat, Brain Res. 113 (1976) 1–19.
[13] A. Peters, B.R. Payne, A numerical analysis of the geniculocortical input to striate cortex in the monkey, Cereb. Cortex 4 (1993) 215–229.
[14] B. Ahmed, J.C. Anderson, K.A. Martin, J.C. Nelson, Polyneuronal innervation of spiny stellate neurons in cat visual cortex, J. Comp. Neurol. 341 (1994) 39–49.
[15] D.H. Hubel, T.N. Wiesel, Uniformity of monkey striate cortex: a parallel relationship between field size, scatter, and magnification factor, J. Comp. Neurol. 158 (1974) 295–305.
[16] J.D. Cowan, A.E. Friedman, Simple spin models for the development of ocular dominance columns and iso-orientation patches, in: R. Lippmann, J. Moody, D. Touretzky (Eds.), Advances in Neural Information Processing, Vol. 3, Morgan Kaufmann, Los Altos, CA, pp. 26–31.
[17] N.V. Swindale, A model for the formation of ocular dominance stripes, Proc. Roy. Soc. London B Biol. Sci. 208 (1980) 243–264.
[18] C. von der Malsburg, Development of ocularity domains and growth behavior of axon terminals, Biol. Cybern. 32 (1979) 49–62.
[19] M.G. Rosa, R. Gattass, M. Fiorani Jr., J.G. Soares, Laminar, columnar and topographic aspects of ocular dominance in the primary visual cortex of Cebus monkeys, Exp. Brain Res. 88 (1992) 249–264.
[20] C.J. Shatz, M.P. Stryker, Ocular dominance in layer IV of the cat's visual cortex and the effects of monocular deprivation, J. Physiol. (London) 281 (1978) 267–283.
[21] P.A. Anderson, J. Olavarria, R.C. Van Sluyters, The overall pattern of ocular dominance band in cat visual cortex, J. Neurosci. 8 (1988) 2183–2200.
[22] J.C. Horton, D.R. Hocking, Intrinsic variability of ocular dominance column periodicity in normal macaque monkeys, J. Neurosci. 16 (1996) 7228–7239.